

# API: Boosting Multi-Agent Reinforcement Learning via Agent-Permutation-Invariant Networks

Xiaotian Hao<sup>1</sup> Weixun Wang<sup>1</sup> Hangyu Mao<sup>2</sup> Yaodong Yang<sup>3</sup> Dong Li<sup>2</sup> Yan Zheng<sup>1</sup> Zhen Wang<sup>4</sup> Jianye Hao<sup>1,2</sup>

## Abstract

Multi-agent reinforcement learning suffers from poor sample efficiency due to the exponential growth of the state-action space. Considering a homogeneous multiagent system, a global state consisting of  $m$  homogeneous components has  $m!$  differently ordered representations, thus designing functions satisfying permutation invariant (PI) can reduce the state space by a factor of  $\frac{1}{m!}$ . However, mainstream MARL algorithms ignore this property and learn over the original state space. To achieve PI, previous works including data augmentation based methods and embedding-sharing architecture based methods, suffer from training instability and limited model capacity. In this work, we propose two novel designs to achieve PI, while avoiding the above limitations. The first design permutes the same but differently ordered inputs back to the same order and the downstream networks only need to learn function mapping over fixed-ordering inputs instead of all permutations, which is much easier to train. The second design applies a hypernetwork to generate customized embedding for each component, which has higher representational capacity than the previous embedding-sharing method. Empirical results on the SMAC benchmark show that the proposed method achieves **100%** win-rates in almost all hard and super-hard scenarios (**never achieved before**), and superior sample-efficiency than the state-of-the-art baselines by up to 400%.

## 1. Introduction

Multi-agent reinforcement learning (MARL) has successfully addressed many complex real-world problems, such as multi-player games (Vinyals et al., 2019; Berner et al.,

2019), autonomous vehicles (Zhou et al., 2020) and robot swarms (Hüttenrauch et al., 2017). But MARL algorithms still suffer from poor sample-efficiency and poor scalability due to the curse of dimensionality, i.e., the joint state-action space grows exponentially as the number of agents increases. The key to solve this problem is to reduce the size of the search space properly (Yang et al., 2021).

In this paper, we focus on the inductive biases of permutation invariance to reduce the state-action space. In MARL, the observation  $o$  is typically represented as a set of components where each component represents each agent’s own features. When the  $m$  components are homogeneous, i.e., semantically same and exchangeable, there are  $m!$  differently ordered permutations of the observation. But they inherently have the same information. Thus, building functions that are insensitive to components’ orders, i.e., differently ordered inputs have the same output (permutation invariant), can significantly reduce the input space by a factor of  $\frac{1}{m!}$  compared to the vanilla permutation sensitive functions.

However, mainstream algorithms, e.g., QMIX (Rashid et al., 2018) and MAPPO (Yu et al., 2021), ignore this property and simply take a fixedly ordered concatenation of the  $m$  components as the input to a permutation sensitive Multi-layer Perceptron (MLP), which is sample inefficient. For example, considering a case of two homogeneous agents, i.e.,  $m = 2$ , each agent has two features ‘A’ and ‘B’. For each agent  $i$ , given  $o_1=[A, B]$  and  $o_2=[B, A]$ , since the 2 agents are exchangeable,  $o_1$  and  $o_2$  are semantically same and thus  $\pi_i(a_i|o_1)$  and  $\pi_i(a_i|o_2)$  should be identical. But feeding these differently ordered observations into an MLP will lead to different outputs. Therefore, at least  $m!$  times more samples are needed to train the MLP such that different permutations of inputs can have the same output. This problem can become significant with the increase of  $m$ .

Two types of methods have been proposed to achieve permutation invariance. The first employs the idea of data augmentation, e.g., Ye et al. (2020) shuffle the order of  $m$  components to generate  $m!$  more data and force these generated data to have the same output through training. However, its policy network is permutation sensitive, thus is inefficient and difficult to train. The second category methods employ naturally permutation invariant architectures to design MARL algorithms, e.g., Li et al. (2021); Liu

<sup>1</sup>College of Intelligence and Computing, Tianjin University <sup>2</sup>Noah’s Ark Lab, Huawei <sup>3</sup>Department of Computer Science and Engineering, The Chinese University of Hong Kong <sup>4</sup>Northwestern Polytechnical University. Correspondence to: Jianye Hao <jianye.hao@tju.edu.cn>.

et al. (2020) and Hu et al. (2021b) apply Deep Sets (Zaheer et al., 2017), GNNs (Battaglia et al., 2018) and Transformer (Vaswani et al., 2017) to MARL respectively. These models incorporate shared input embedding layers, pooling layers to achieve permutation invariance. But the limited representational capacity of the shared embedding layers may result in poor performance (Wagstaff et al., 2019).

In this work, our major contributions are two novel Agent Permutation Invariant (API) designs which significantly boost the performance of existing mainstream MARL methods, while avoiding the defects of previous methods mentioned above. Instead of doing data augmentation or modifying the architectures of the original MARL methods, we first propose a Deep Permutation Network (DPN) which explicitly removes the influence of the input order by data preprocessing. Specifically, we generate permutation matrices to explicitly permute the semantically same but differently ordered input sets into a fixedly ordered one. Then any existing MARL method can be directly applied downstream without modification. And they only need to learn function mapping over fixed-ordering inputs (much smaller space) instead of over all permutations of inputs compared with data augmentation based methods. Thus it is easier to train.

One limitation of DPN is that for some special input cases, DPN may suffer from training instability issue. Thus, to more stably achieve API while ensuring the representational capacity, we propose a novel HyPerNetwork based API architecture: HPN. Specifically, we maintain a hypernetwork to separately generate the weights of the input embedding layer for each component by taking its own feature as input. Therefore, compared with previous Deep Sets, GNNs or Transformer based architectures which use shared embedding weights, our model’s representational capacity has been substantially improved since any difference in each component’s feature will result in different embedding weights. Then we merge these individually embedded components by sum pooling and thus make the model permutation invariant.

Besides, for many functions in MARL tasks, the outputs have semantic meanings and there exist one-to-one correspondences between the components of the function output and input. Take  $Q_i(a_i|o_i)$  of the typical Starcraft Multi-Agent Challenge (SMAC) benchmark (Samvelyan et al., 2019) for an example, there exist one-to-one correspondences between the ‘enemies’ of the input  $o_i$  and ‘attack actions’ of the Q-value output. For these functions, the outputs should be permutation equivariant with respect to the input components. Therefore, we also exploit the Agent Permutation Equivariance (APE) property when design our DPN and HPN architectures. We conduct comprehensive evaluations on SMAC, and our approach achieves **100%** win-rates in almost all hard and super-hard scenarios, which has **never achieved before** to the best of our knowledge. Moreover,

our approach demonstrates superior sample-efficiency than state-of-the-art baselines by up to 400%. Lastly, we conduct detailed ablation studies to investigate the importance of each submodules of our approach. The code is available at <https://github.com/TJU-DRL-LAB/API-MARL>.

## 2. Background

### 2.1. Multiagent Markov Decision Process

Multiagent Markov Decision Process (MMDP, also know as Markov game) (Littman, 1994) is an extension of MDP to multi-agent settings. An MMDP is defined as a tuple  $\langle \mathcal{N}, \mathcal{S}, \mathcal{O}, \mathcal{A}, P, r, Z, \gamma \rangle$ .  $\mathcal{N}$  is a set of  $n$  agents.  $\mathcal{S}$  is the set of global states.  $\mathcal{O} \equiv \{\mathcal{O}_1, \dots, \mathcal{O}_n\}$  denotes the observation space for  $n$  agents.  $\mathcal{A} \equiv \mathcal{A}_1 \times \dots \times \mathcal{A}_n$  is the joint action space, where  $\mathcal{A}_i$  is the set of actions that agent  $i$  can take. At each step, each agent  $i$  receives a private observation  $o_i \in \mathcal{O}_i$  according to the observation function  $Z(s, \mathbf{a}) : \mathcal{S} \times \mathcal{A} \rightarrow \mathcal{O}$  and produces an action  $a_i \in \mathcal{A}_i$  by a policy  $\pi_i(a_i|o_i)$ . All individual policies constitute the joint policy  $\pi = \pi_1 \times \dots \times \pi_n$ . Then the game transits to the next state  $s'$  according to the transition function  $P(s'|s, \mathbf{a})$ , where  $\mathbf{a} \in \mathcal{A}$  is the joint action. Each agent  $i$  receives a reward according to the reward function  $r \equiv \{r_1, \dots, r_n\}$ . The target of each agent is to learn an optimal policy  $\pi_i^*$  which could maximize its expected return  $R_i = \sum_{t=0}^T \gamma^t r_i(s^t, a^t)$ , where  $\gamma$  is a discount factor and  $T$  is the time horizon.  $Q_i^{\pi_i}(o_i, a_i) = \mathbb{E}_{\pi_i, P}[R_i|o_i, a_i]$  and  $V_i^{\pi_i}(o_i) = \mathbb{E}_{\pi_i, P}[R_i|o_i]$  denote each agent  $i$ ’s individual Q and V functions. The joint Q and V functions are denoted as  $Q_{\pi}(s, \mathbf{a}) = \mathbb{E}_{\pi, P}[R|s, \mathbf{a}]$  and  $V_{\pi}(s) = \mathbb{E}_{\pi, P}[R|s]$  respectively. When the environment is partially observable, the problem is formulated as Decentralized Partially Observable MDP (Dec-POMDP) (Oliehoek & Amato, 2016).

### 2.2. Permutation Invariance and Equivariance

**Permutation Invariant Function.** A function  $f : X \rightarrow Y$  where  $X = [x_1, x_2, \dots, x_m]^T$  of size  $(m, k)$  is a set consisting of  $m$  components (each of which is of dimension  $k$ ), is said to be permutation invariant if permutation of the input components does not change the output of the function (Kalra et al., 2020). Mathematically,

$$f([x_1, x_2, \dots, x_m]^T) = f(M[x_1, x_2, \dots, x_m]^T)$$

where  $M$  is a permutation matrix of size  $(m, m)$ , which is a binary matrix that has exactly a single unit value in every row and column and zeros everywhere else.

**Permutation Equivariant Function.** Similarly, a function  $f : X \rightarrow Y$  is permutation equivariant if permutation of input components permutes the output components with the same matrix  $M$  (Kalra et al., 2020). Mathematically,

$$f(M[x_1, x_2, \dots, x_m]^T) = M[y_1, y_2, \dots, y_m]^T$$

In deep learning, the Multilayer Perceptron (MLP) is permutation sensitive function, Deep Set (Zaheer et al., 2017) is permutation invariant function and the Self-Attention Layer (Vaswani et al., 2017) is permutation equivariant function. In MARL, the state or observation is usually represented as a set of  $m$  components:  $[x_1, \dots, x_m]$ . Each component  $x_i \in \mathcal{X}$  is a vector of dimension  $k$ , which represents an atomic semantic meaning, e.g., agent  $i$ 's own features.  $\mathcal{X}$  is the feature space. Because permuting the orders of the  $m$  components does not change the information of the set, we can leverage the permutation invariance and permutation equivariance properties to design more sample efficient models. We will detail this in Section 3 and Section 4.

### 3. Related Work

**Concatenation.** The mainstream algorithms, e.g., VDN (Sunehag et al., 2017), QMIX (Rashid et al., 2018), MADDPG (Lowe et al., 2017) and MAPPO (Yu et al., 2021), simply represent the set input as a concatenation of features of the  $m$  components in a user-specified order  $[x_1, \dots, x_m]$ . For these methods, feeding a permuted input will result in a different output, so the search space is  $|\mathcal{X}|^m$ . Although these methods use inefficient representations of the input set, they achieve SOTA performance on some benchmarks.

**Experience Augmentation.** Since at least  $|\mathcal{X}|^m$  samples are needed to train the concatenation based methods, Ye et al. (2020) propose an experience augmentation method that generates more training data by shuffling the order of  $[x_1, \dots, x_m]$  and additionally updates the model parameters based on the generated experiences. They apply experience augmentation to MADDPG and achieve better performance and faster convergence speed. However, the shuffling method needs to augment  $m! - 1$  new data for each sample, which is computational expensive (Wadhwanian et al., 2019). Besides, these generated differently ordered experiences have the same information and thus should have the same Q-value as the original one. But it is inefficient to train a permutation-sensitive function, e.g., MLP, to output the same value when taking differently ordered features as inputs, which may lead to poor estimation accuracy.

**Deep Set & Graph Neural Network.** Instead of doing data augmentation, Deep Set (Zaheer et al., 2017) constructs a family of permutation invariant neural architectures for learning set representations. Each entity  $x_i$  is mapped separately to some latent space  $\phi(x_i)$  using a shared network. These latent representations are then passed through a permutation invariant pooling layer (e.g. sum, mean, or max) to ensure the permutation-invariance of the whole function, e.g.,  $f(X) = \rho(\sum_{i=1}^m \phi(x_i))$ , where  $\rho$  is usually a nonlinear activation. Similarly, Graph Neural Networks (GNNs) (Veličković et al., 2018; Battaglia et al., 2018) also adopt shared embedding and pooling layers to learn functions on

graphs. Wang et al. (2020b); Li et al. (2021) and Jiang et al. (2018); Liu et al. (2020) have applied Deep Set and GNN to MARL. However, due to the limited representational capacities of the shared embedding  $\phi(x_i)$ , the performance is usually limited (Wagstaff et al., 2019). Besides, these works do not consider the permutation equivariance property.

**Multi-head Self-Attention & Transformer.** Most recently, Hu et al. (2021b) adopt transformer-based (Vaswani et al., 2017) model to MARL and propose Universal Policy Decoupling Transformer (UPDeT), which employs the multi-head self-attention mechanism to process every element  $x_i$  of the input set and outperforms conventional RNN-based methods (Rashid et al., 2018). Transformer could be considered as a special case of Graph Attention Network (GAT, a kind of GNN) (Veličković et al., 2018) which uses a fully connected adjacency matrix. Although UPDeT implicitly takes the permutation invariance and permutation equivariance into consideration, the performance is still limited due to the use of the shared embedding  $\phi(x_i)$ .

### 4. Motivation

In MARL, the environments typically consist of  $m$  components, including  $n$  learning agents and  $m - n$  non-player characters (NPCs). Therefore, the states and observations are factorizable as sets of  $m$  components  $[x_1, \dots, x_m]$ . Each component  $x_i \in \mathcal{X}$  is a vector of dimension  $k$ , representing each agent's or NPC's own features.  $\mathcal{X}$  is the feature space.

**Agent Permutation Invariance (API).** For homogeneous settings, i.e., the  $m$  components belong to the same type, have identical feature spaces, action spaces and reward functions, the positions of the components are exchangeable. The size of an *fixedly ordered representation* is  $|\mathcal{X}|^m$ . Instead, using a *permutation invariant representation*, i.e., removing the influence of the input order, can reduce the size of the input space by a factor of  $\frac{1}{m!}$ . As the number of  $m$  increases, the removal of these redundancies results in a much smaller search space, upon which we could more easily learn a policy. As shown in Figure 1, taking  $Q_i(a_i|o_i)$  of SMAC as an example, the input set  $o_i = [x_1, \dots, x_m]$  can be divided into 2 groups: an ally group  $o_i^{\text{ally}}$  and an enemy group  $o_i^{\text{enemy}}$ . The output action Q-values can be divided into 2 groups as well: Q-values for move actions  $\mathcal{A}_i^{\text{move}}$  and attack actions  $\mathcal{A}_i^{\text{attack}}$ . Given the same  $o_i$  with different orders, the Q-values of  $\mathcal{A}_i^{\text{move}}$  should be the same and thus  $Q_i(\mathcal{A}_i^{\text{move}}|o_i)$  should be permutation invariant. Note that if the components are not homogeneous, we can divide the components into multiple groups such that components within the same group are homogeneous. Thus the search space can still be reduced by incorporating permutation invariant representation within each homogeneous group.

**Agent Permutation equivariance (APE).** In MARL tasks,

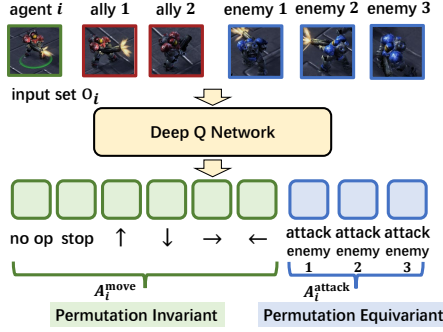


Figure 1. API and APE individual  $Q_i(a_i|o_i)$  function in SMAC.

the outputs of many functions have semantic meanings and there exist one-to-one correspondences between the components of the function output and function input. Again taking  $Q_i(a_i|o_i)$  in SMAC as an example, since there is a one-to-one correspondence between each ‘attack’ action in  $\mathcal{A}_i^{\text{attack}}$  and each entity in  $o_i^{\text{enemy}}$ , the Q-values of  $\mathcal{A}_i^{\text{attack}}$  should be equivariant to the permutations of entities in  $o_i^{\text{enemy}}$ . Overall, both the API and APE properties can be exploited to design more sample efficient methods in MARL.

## 5. Methodology

In this section, we propose two approaches which can be easily integrated into existing MARL algorithms to efficiently achieve API and APE without losing the representational capacity of the neural networks. As mentioned before, previous data augmentation based methods (Ye et al., 2020) transform existing permutation-sensitive networks, e.g. MLPs, to approximately achieve permutation invariant. They use *random permutation matrix* to randomly shuffle the order of the input components to generate more training data (enlarge the dataset) and force these augmented data to approximately have the same output through training. But it is hard to train differently ordered inputs to have a same output. Instead, we generate *inverse permutation matrix* to permute the same but differently ordered input sets back into the one arranged in the same order (reduce the feature/input space). These generated permutation matrices play the role of ensuring permutation invariant. Then, any mainstream ‘concatenation’ based method can be immediately integrated downstream without modification. They only need to learn function mapping over fixed-ordering inputs (a much smaller input space), which is much easier to train against the data augmentation based methods. Besides, compared with Deep Set and GNN based methods, we do not rely on a shared embedding function  $\phi(x_i)$  to ensure API, thus the representational capacity is not limited.

### 5.1. API Deep-Permutation-Network (API-DPN)

API-DPN can easily convert any mainstream method to be both API and APE. The core idea is that given a input set

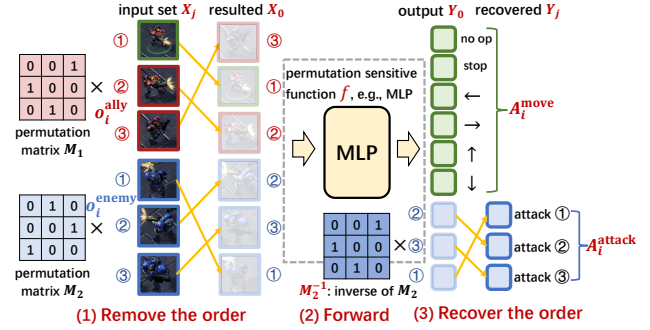


Figure 2. We take the  $Q_i(a_i|o_i)$  of SMAC as an example to illustrate the 3 steps of API-DPN, which can transform any permutation-sensitive function, e.g., MLP, to be both API and APE.

$X_j = [x_1, \dots, x_m]^T$  of size  $(m, k)$  arranged by any order  $j \in [0, m!]$ , we first generate a permutation matrix  $M_j$  to transform  $X_j$  into a fixedly ordered  $X_0$ , i.e.,  $M_j X_j = X_0$ . Then any permutation-sensitive functions can be directly applied downstream. In summary, there are 3 steps to convert a method to be both API and APE, which is shown schematically in Figure 2.

(1) **Remove the order:** For any input set  $X_j$ , we generate a permutation matrix  $M_j$  and permute  $X_j$  to a fixedly ordered  $X_0$ . In the example of Figure 2, we separately generate two permutation matrices  $M_1$  and  $M_2$  to permute differently ordered  $o_i^{\text{ally}}$  and  $o_i^{\text{enemy}}$  into fixedly ordered ones. How to generate the matrix will be introduced later in details.

(2) **Forward:** Since  $X_0$ ’s order is fixed, any function  $f$  could be applied downstream. We denote the output of function  $f$  as  $Y_0 = f(X_0) = f(M_j X_j)$ . So far, the output  $Y_0$  is permutation invariant with the input  $X_j$ . In Figure 2, we feed the permuted  $o_i^{\text{ally}}$  and  $o_i^{\text{enemy}}$  into an MLP and get the output Q-values of  $\mathcal{A}_i^{\text{move}}$  and  $\mathcal{A}_i^{\text{attack}}$ , which are API.

(3) **Recover the order:** If there is a one-to-one correspondence between the components in  $Y_0$  and  $X_j$ , an additional inverse permutation step is performed to recover the initial order and to keep the function permutation equivariant, i.e.,  $Y_j = M_j^{-1} Y_0 = M_j^{-1} f(M_j X_j)$ . In the example, an inverse permutation matrix  $M_2^{-1}$  is applied to Q-values of  $\mathcal{A}_i^{\text{attack}}$  to achieve permutation equivariant.

**Permutation Matrix Generation.** The remaining problem is how to generate  $M_j$  such that  $M_j X_j = X_0, \forall j \in [0, m!]$ . This problem has been studied in Vision domain and is called Permutation Learning, Matching Learning or Assignment Learning (Santa Cruz et al., 2017; 2018; Mena et al., 2018). The core is learning to assign each component  $x_i$  of the input set  $X_j$  to the correct position. In our setting, directly applying previous solutions does not behave very well, which will be discussed in Appendix B.2. Thus, we propose a new end to end differentiable sequential assignment solution. Because  $X_0$  is fixed and the  $d$ -th row of  $X_0$  only depends on the  $d$ -th row of  $M_j$  (i.e.,  $X_0[d] = M_j[d] X_j$ ),



**Algorithm 1** Permutation Matrix Generation.

```

1: Input:  $X_j$  of size  $(m, k)$ , temperature coefficient  $\tau$ ;
2: Output: permutation matrix  $M_j$ ;
3:  $L_j = \text{MLP}_\theta(X_j)$ ; //  $L_j$  is of size  $(m, m')$ ;
4:  $\hat{L}_j = L_j^T$ ; // transpose  $L_j$  to  $\hat{L}_j = \mathbb{R}^{m' \times m}$ .
5: assignment = [ ];
6: invalid_mask = [0, 0, ..., 0]; // init to zeros.
7: for each row  $d = 0, 1, \dots, m'-1$  of  $\hat{L}_j$  do
8:   logit =  $\hat{L}_j[d, :]$ ;
9:   negative_mask = invalid_mask * (-1e10);
10:  masked_logit = logit + negative_mask;
11:  assign = gumbel_softmax(masked_logit,  $\tau$ , hard=True);
12:  invalid_mask += assign; // make the positions of previously assigned  $x_i$ s become invalid.
13:  assignment.append(assign);
14: end for
15:  $M_j = \text{stack}(\text{assignment}, \text{dim}=0)$ ; // of size  $(m', m)$ .
16: return  $M_j$ ;
    
```

we can sequentially generate each row of  $M_j$ .

The full algorithm is shown in Algorithm 1. Given  $X_j$  of size  $(m, k)$ , which can be viewed as a batch of  $m$   $x_i$ s each of which is of dimension  $k$ , we first feed all  $x_i$ s into a shared  $\text{MLP}_\theta$  whose input dimension is  $k$  and output dimension is  $m$  (line 3). **To avoid confusion, we mark the output dimension  $m$  as  $m'$  in the following paper** (including Algorithm 1). We get the output logits of the MLP as  $L_j = \mathbb{R}^{m \times m'}$ , where the  $d$ -th column of  $L_j$  reflects the probabilities of assigning different  $x_i$ s to the same  $d$ -th row of  $X_0$ . Then, we transpose  $L_j$  to  $\hat{L}_j = \mathbb{R}^{m' \times m}$  (line 4) such that the  $d$ -th row of  $\hat{L}_j$  will play the same role as the  $d$ -th row of  $M_j$  except for not being a valid permutation matrix, i.e., the probabilities should be either 0 or 1. Thus, we then convert  $\hat{L}_j$  into a valid permutation matrix  $M_j$  (line 5-15) by sequentially converting each row of  $\hat{L}_j$  into a one-hot vector through Gumbel softmax<sup>1</sup> (Jang et al., 2016) (line 11) while keeping the conversion differentiable. To ensure that one  $x_i$  can only be assigned to one position, an invalid mask (line 6) is utilized to record the positions of  $x_i$ s that have been assigned previously (marked as invalid  $x_i$ s). Then, a negative mask (line 9) is generated to ensure the probabilities of picking these invalid  $x_i$ s are 0.

Two permutation matrix generation examples are shown schematically in Figure 3, of which the input sets are the same but arranged in different orders. In Figure 3, each  $x_i$  and each row of logits  $L_j$  are marked in different shades of blue. The logits  $L_j$  of size  $(m, m')$  is firstly transposed into  $\hat{L}_j$  of size  $(m', m)$ . Then  $\hat{L}_j$  is converted into  $M_j$  through Gumbel softmax row by row. From the examples, we see

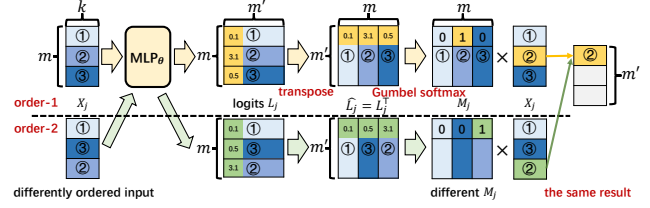


Figure 3. Two examples of the sequential generation of each row of  $M_j$ . Differently ordered inputs result in the same output.

that given the MLP’s parameter  $\theta$ , Algorithm 1 can sequentially generate each row of  $M_j$  such that for  $\forall j \in [0, m!)$ ,  $M_j X_j$  results in the same  $X_0^\theta$ .  $X_0^\theta$  means the components’ order of  $X_0$  only depends on the MLP’s parameter  $\theta$ . Different  $\theta$ s will result in different  $X_0$ s. Thus our target is to update the parameter  $\theta$  of the MLP such that the resulted  $X_0$  can achieve smaller RL loss, i.e., the MLP is trained in an end-to-end fashion according to the RL loss function.

**Limitation of DPN.** When applying DPN to mainstream algorithms, e.g., VDN, QMIX or MAPPO, after removing the components’ order of  $X_j$  by  $X_0^\theta = M_j X_j$ ,  $X_0^\theta$  will be firstly fed into a fully connected (FC) layer. An FC layer under the submodular view is shown in Figure 4 (a). Feeding a concatenated  $[x_1, \dots, x_m]$  into an FC layer can be seen as that (1) each element  $x_i$  is first separately embedded by a different matrix  $W_i$ <sup>2</sup>; (2) the embedding of each  $x_i$  as well as the bias  $b$  are summed together to get the output, i.e.,  $\text{output} = \sum_{i=0}^{m-1} x_i W_i + b$ . Taken together, the training of  $\text{MLP}_\theta$  of Algorithm 1 can be viewed as learning to permute  $X_j$  into the best  $X_0^\theta$  such that each  $x_i$  will be assigned with the most suitable  $W_i$ . A prior is that to stabilize and facilitate training, the same  $x_i$  should be assigned with the same  $W_i$ . But the number of candidate  $W_i$ , i.e., the submodule number, is limited to  $m$ , which results in two bad cases: (1) For the same input set  $[x_1, \dots, x_m]$ , although  $x_i = x_j$ , they must be assigned to different  $W_i$ s; (2) For the same  $x_i$  appeared in different input sets, for the reason that  $x_{-i}$ s are different, the same  $x_i$  may also be assigned with different  $W_i$ s. All these will disturb the learning process.

## 5.2. API-HyperNetwork (API-HPN)

To address the limitation of API-DPN and make it easier to keep API and APE while improving the representational capacity, we propose a more flexible hypernet-based architecture: API-HPN. API-HPN incorporates hypernetworks (Ha et al., 2016) to generate different weights  $W_i$ s for different input components  $x_i$ s to improve representational capacity while ensuring the same  $x_i$  always be assigned with the same weight  $W_i$  even in the above two bad cases. In this way, the learning stability could be substantially improved. The architecture of our API-HPN is shown in

<sup>1</sup>Details of Gumbel softmax is shown in Appendix B.1.

<sup>2</sup>Note that compared with Deep Set, GNN and Transformer, this input embedding function is not shared.

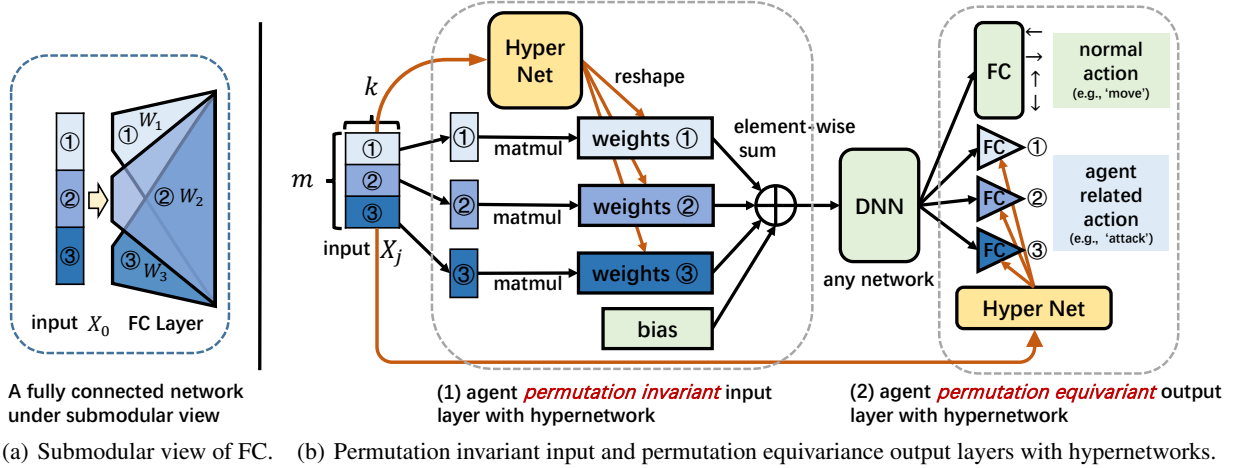


Figure 4. Agent permutation invariant network with hypernetworks.

Figure 4 (b). We also take the  $Q_i(a_i|o_i)$  as an example. The model mainly composes of two modules:

**Agent Permutation Invariant Input Layer.** Hypernetworks (Ha et al., 2016; Sarafian et al., 2021) are a family of neural architectures which use one network, known as hypernetwork, to generate the weights for another network. In our setting, the hypernetwork is utilized to generate a different  $W_i$  for each  $x_i$  of the input set  $X_j$ . As shown in Figure 4 (b),  $X_j$  (which can be viewed as a batch of  $m$   $x_i$ s each of which is of dimension  $k$ , represented by different shades of blue) is firstly fed into a shared hypernetwork (marked in yellow), whose input size is  $k$  and output size is  $k * h$ . Then, the corresponding outputs are reshaped to  $[k, h]$  and serve as the submodule weights  $W_i$ s of the normal FC layer (see Figure 4 (a)). Note that different  $x_i$ s will generate different  $W_i$ s and the same  $x_i$  will always correspond to the same  $W_i$ , thus the limitation of API-DPN is eliminated. Then, each  $x_i$  is multiplied by  $W_i$  and all multiplication results and the bias  $b$  are summed together to get the output. Since each element  $x_i$  is processed separately by its corresponding  $W_i$  and then merged by a permutation invariant ‘sum’ function, the permutation invariance is reserved.

**Agent Permutation Equivariance Output Layer.** Similarly, to keep the whole network permutation equivariance, the submodular weights and bias of the agent-related actions in the output layer, e.g.,  $\mathcal{A}_i^{\text{attack}}$  of SMAC, are also generated by a hypernetwork. As mentioned above, the input  $x_i$  and output  $W_i$  of the hypernetwork always correspond one-to-one, so the input order change will result in the same output order change, thus achieving permutation equivariance.

Finally, we emphasize that both API-DPN and API-HPN are general designs and can be easily integrated into existing MARL algorithms to boost the learning speed as well as the converged performance. All parameters of API-DPN and API-HPN are simply trained end-to-end with backpropagation according to the corresponding RL loss function.

## 6. Experiments

In this section, we study the following research questions (RQs) via comprehensive experiments.

**RQ1 (Comparison with SOTA):** Can API-HPN improve the learning efficiency and outperform the previous SOTA approach?

**RQ2 (Performance):** Do API-HPN outperform related baselines that consider the permutation invariance and the permutation equivariant property?

**RQ3 (Superiority of API-HPN):** Does API-HPN further improve the learning stability as well as the converged performance compared with API-DPN?

**RQ4 (Network Size):** For API-HPN, incorporating a hypernetwork results in a ‘bigger’ model. Can we achieve better results by simply increasing the network size?

**RQ5 (Necessity of APE):** Whether keeping the output layer permutation equivariant is beneficial?

**RQ6 (Representational Capacity):** Whether improve representational capacity of the API input embedding layer, i.e., using different  $\phi_i(x_i)$ s for different  $x_i$ s is beneficial?

### 6.1. Experimental Setups

**StarCraft Multi-Agent Challenge.** We mainly evaluate our methods in the challenging StarCraft II micromanagement benchmark (SMAC) (Samvelyan et al., 2019), which has become a commonly-used testbed for MARL algorithms (Rashid et al., 2018; Wang et al., 2019; Rashid et al., 2020; Hu et al., 2021b;a). SMAC consists of a set of StarCraft II micro battle scenarios, where units are divided into 2 teams: allies and enemies. The ally units are controlled by the learning agents while the enemy units are controlled by the built-in handcrafted rules. The agents receive observations containing distance, relative location, health, shield, and type of units within the sight range. The goal is to train the learning agents to defeat the enemy units. In SMAC, all scenarios are classified into Easy, Hard, and Super Hard

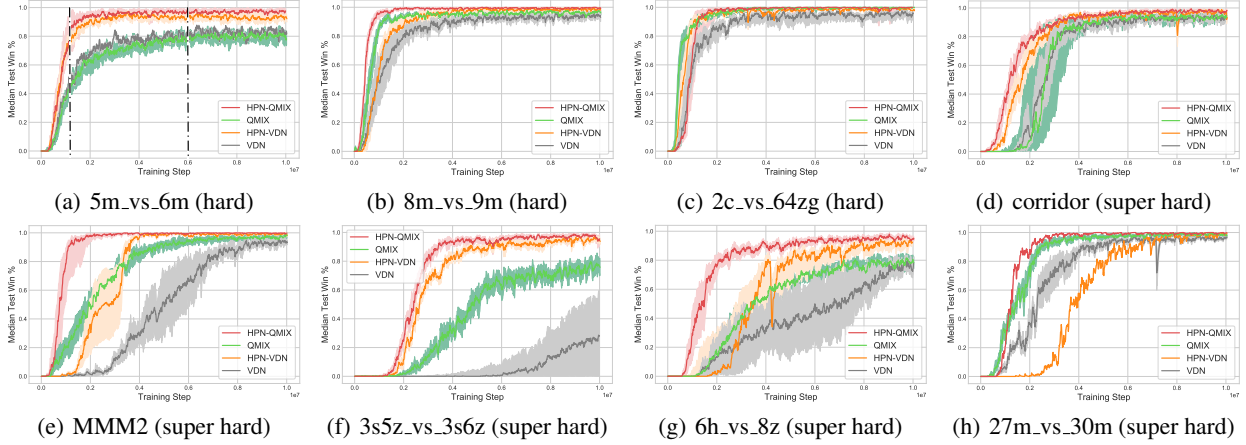


Figure 5. The learning curves of our HPN-QMIX and HPN-VDN compared with the SOTA fine-tuned QMIX and the fine-tuned VDN.

levels. Almost all scenarios contain homogeneous agents, thus SMAC is suitable for agent permutation invariant study. For the reason that the Easy scenarios can be effectively solved by existing methods (Hu et al., 2021a), we mainly evaluate our methods in all Hard and Super Hard scenarios.

**Evaluation Metric.** Following Rashid et al. (2018); Samvelyan et al. (2019); Hu et al. (2021a), our evaluation metric is the function that maps the environment steps to winning percentage throughout training. For each experiment, we run 32 test episodes without exploration to record the test win rate. Each experiment is repeated using 5 independent training runs and the resulting plots include the median performance as well as the 25%-75% percentiles.

**Previous SOTA & Code Implementation.** Recently, Hu et al. (2021a) have demonstrated that the code-level implementation really matters in Deep MARL. They propose **fine-tuned QMIX** by incorporating code-level optimizations into QMIX (Rashid et al., 2018), e.g., TD-lambda, Adam optimizer and large epsilon annealing steps, which outperforms the original QMIX, Qatten (Yang et al., 2020), Weighted QMIX (Rashid et al., 2020), QPLEX (Wang et al., 2020a) and achieves SOTA performance in SMAC. We follow the hyperparameter settings of fine-tuned QMIX and implement the code based on their official open source project PyMARL2<sup>3</sup>. The detailed hyperparameter settings of all methods are given in Appendix C.

## 6.2. Comparison with SOTA (RQ1)

Here, we compare our API-HPN with the SOTA fine-tuned QMIX (Hu et al., 2021a) and the fine-tuned VDN. We apply our API-HPN architecture to the individual Q-network of the fine-tuned QMIX and VDN and denote them as HPN-QMIX and HPN-VDN respectively. The learning curves over 8 hard and super hard scenarios are shown in Figure 5. Note that we do not extremely tune the hyperparameters for

each scenario and use the same parameter settings across all scenarios instead. From the figure, we conclude that:

- (1) Our HPN-QMIX surpasses the fine-tuned QMIX by a large margin and achieves 100% test win rates in almost all scenarios, especially in *5m\_vs.6m*, *3s5z\_vs.3s6z* and *6h\_vs.8z* (never achieved before). Therefore, HPN-QMIX achieves the **new SOTA** on the SMAC benchmark;
- (2) Our HPN-VDN also significantly improves the performance of the fine-tuned VDN, and it even surpasses the fine-tuned QMIX in most scenarios and achieves close performance to the HPN-QMIX, which minimizes the gaps between the VDN-based and QMIX-based algorithms;
- (3) The sample efficiency of both HPN-VDN and HPN-QMIX is significantly improved, especially in *5m\_vs.6m*, *MMM2*, *3s5z\_vs.3s6z* and *6h\_vs.8z*. An example is shown in Figure 5 (a), on *5m\_vs.6m*, we mark 2 dotted lines in black to indicate the number of training steps needed to achieve the same 80% win rate of different algorithms. We see HPN-VDN and HPN-QMIX use much less samples by a factor of  $\frac{1}{4}$ . The full results on all hard and super hard scenarios are shown in Figure 8 of Appendix A.1.

## 6.3. Comparison with Related Baselines (RQ2)

The baselines we compared are:

- (1) **Experience Augmentation (EA)** (Ye et al., 2020): we apply EA to QMIX (denoted as EA-QMIX) by generating more training data through shuffling the input order and using the generated data to additionally update the parameters.
- (2) **Deep Set**: Similar to Li et al. (2021), we apply Deep Set to the individual Q-network of QMIX (denoted as SET-QMIX), i.e., all  $x_i$ s use a shared embedding layer and then aggregated by sum pooling, to achieve permutation invariant (but not permutation equivariant).
- (3) **GNN**: Following PIC (Liu et al., 2020), we apply GNN to the individual Q-network of QMIX (denoted as GNN-

<sup>3</sup><https://github.com/hijkzzz/pymarl2>



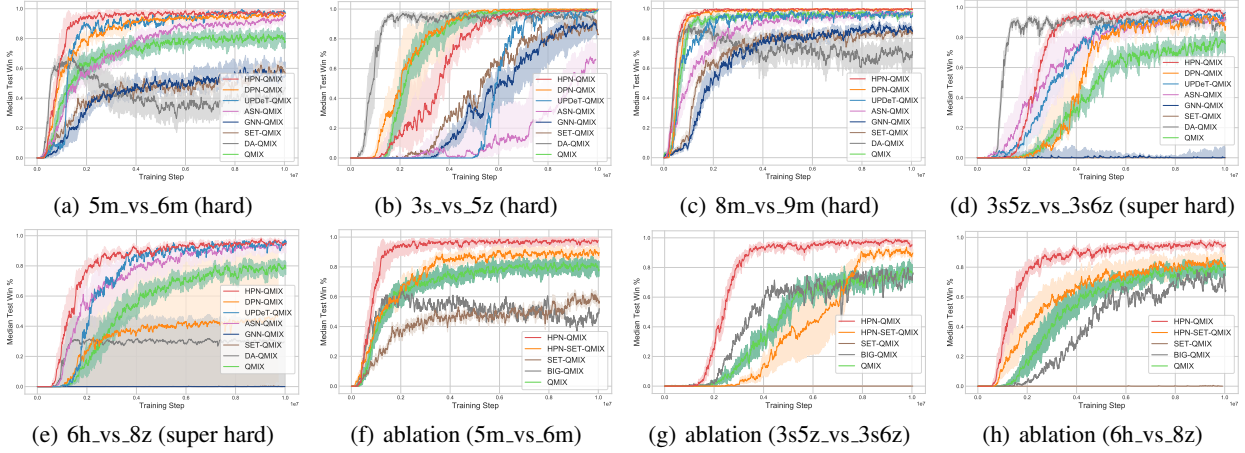


Figure 6. (a)-(e): Comparisons of different methods considering the permutation invariance and equivariance; (f)-(h): Ablation studies.

QMIX) to achieve permutation invariant (but not permutation equivariant).

(4) **ASN** (Wang et al., 2019): ASN characterizes different actions’ influence on other agents based on the action semantics (e.g., move or attack others), which is similar to the permutation equivariance property considered in this paper. We apply ASN to QMIX (denoted as ASN-QMIX).

(5) **UPDeT** (Hu et al., 2021b): a recently representative MARL algorithm based on Transformer which implicitly takes the permutation invariance and permutation equivariance into consideration. We use their official open-source code and apply it to QMIX (denoted as UPDeT-QMIX).

Implementation details of these methods are shown in Appendix B.3. The results are shown in Figure 6 (a)-(e), which indicate that: (1) our HPN-QMIX achieves the best win rates compared with all baselines; (2) EA-QMIX improves both the learning speed and converged performance of QMIX in *3s\_vs\_5z* and *3s5z\_vs\_3s6z* through more times of parameter updating. However, it’s learning process is unstable and collapses in all other scenarios due to the perturbation of the input features, which validates that it is hard to train a permutation-sensitive function (e.g., MLP) to output the same value when taking different orders of features as inputs. (3) SET-QMIX and GNN-QMIX achieve similar performance. Although permutation invariant is maintained, SET-QMIX and GNN-QMIX perform worse than vanilla QMIX, (especially on *3s5z\_vs\_3s6z* and *6h\_vs\_8z*, the win rates are almost 0%). This confirms that the use of a shared embedding layer  $\phi(x_i)$  for each component  $x_i$  limits the representational capacities and restricts the final performance. (4) ASN-QMIX achieves comparable win rates in most scenarios except for *3s\_vs\_5z*, which indicates that considering the permutation equivariance is important. (5) Although UPDeT utilizes multi-head attention to improve the representational capacity of the model, the performance is still worse than our hypernetwork-based HPN-QMIX. The per-

formance drop may be induced by the shared token embedding layer. Note that in the main paper, we only present the results of these methods equipped with QMIX due to the space limit. VDN-based results are shown in Appendix A.2.

#### 6.4. Superiority of API-HPN to API-DPN (RQ3)

The results of the fine-tuned QMIX equipped with API-HPN and API-DPN are shown in Figure 6 (a)-(e), denoted as HPN-QMIX and DPN-QMIX respectively. HPN-QMIX utilizes more flexible hypernetworks to achieve permutation invariant and equivariant with strong representational capacity, while DPN-QMIX explicitly uses permutation matrices to rearrange the order of the input. As discussed in the end of Section 5.1, API-DPN may suffer from some bad cases which disturb the learning process. The results in Figure 6 (a)-(e) show that, (1) both HPN-QMIX and DPN-QMIX achieve superior performance, which validates the effectiveness of our API and APE design; (2) HPN-QMIX is more stable and achieves better win rates than DPN-QMIX, especially in the *6h\_vs\_8z* scenario, which validates the robustness and superiority of our HPN design. Note that we only present the results of API-Networks equipped with QMIX due to the space limit. The results of API-Networks equipped with VDN are shown in Appendix A.2.

#### 6.5. Ablation: Enlarging the Network Size (RQ4)

To make a more fair comparison, we enlarge the agent network of vanilla QMIX (denoted as BIG-QMIX) such that the number of parameters is larger than our HPN-QMIX. The detail number of parameters are shown in Table 2 of Appendix A.3. The results are shown in Figure 6 (f)-(h). We see that simply increasing the parameter number cannot achieve better performance; in contrast, it may even result in worse performance. Similar comparison results of VDN-based methods are also shown in Appendix A.3.



## 6.6. Ablation: APE & Representation Capacity (RQ5/6)

**RQ5:** To validate the importance of the permutation equivariant output layer, we add the hypernetwork-based output layer of HPN to SET-QMIX (denoted as HPN-SET-QMIX). The results are shown in Figure 6 (f)-(h). We see that incorporating an APE output layer could significantly boost the performance of SET-QMIX and the converged performance of HPN-SET-QMIX is superior to the vanilla QMIX. **RQ6:** However, due to the limit representational capacity of the shared embedding layer of Deep Set, the performance of HPN-SET-QMIX is still worse than our HPN-QMIX. Note that the only difference between HPN-QMIX and HPN-SET-QMIX is the input layer, e.g., using hypernetwork-based customized embeddings or a simply shared one. The results validate the importance of improving the representational capacity of the permutation invariant input layer.

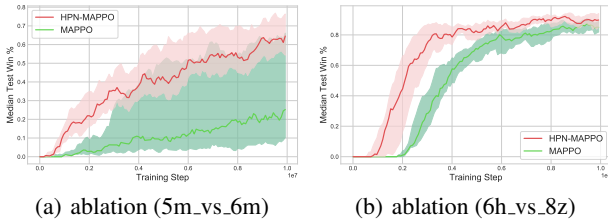


Figure 7. Comparison of HPN-MAPPO with vanilla MAPPO.

## 6.7. Applying API to MAPPO

Besides value-based methods, we further apply API-HPN to policy-based MAPPO (Yu et al., 2021) (denoted as HPN-MAPPO). The results are shown in Figure 7. HPN-MAPPO and vanilla MAPPO are the same except that HPN-MAPPO incorporates API-HPN architecture to achieve API and APE. We see HPN-MAPPO achieves better win rates than vanilla MAPPO, which validates that our API and APE designs are applicable to wide types of MARL methods.

## 7. Discussion

Before we wrap up, let’s quickly review the advantages and disadvantages of different methods which leverage the ‘permutation’ property to design MARL algorithms. The full comparison results are summarized in Table 1.

**(1) Data augmentation based methods.** Data augmentation based methods (Ye et al., 2020) simply adopt the same permutation sensitive networks, e.g., MLPs, as the concatenation based methods (Lowe et al., 2017) (don’t have to modify the network architecture). They approximately achieve API by generating more differently ordered training data and forcing these data to approximately have the same output through training. The advantage is that the network structure is not limited, i.e., do not rely on a shared embedding  $\phi(x_i)$  to ensure API. But it is difficult to train the

Model	API?	APE?	modified architecture?	shared $\phi(x_i)$ ?
Simple Concatenation	✗	✗	✗	✗
Data Augmentation	✗	✗	✗	✗
Deep Set	✓	✗	✓	✓
GNN	✓	✓	✓	✓
Transformer	✓	✓	✓	✓
API-DPN (Ours)	✓	✓	✗	✗
API-HPN (Ours)	✓	✓	✓	✗

Table 1. A comparison on algorithmic properties of existing MARL methods which consider the ‘permutation’ property.

differently ordered inputs to have a same output and thus the API cannot be guaranteed (marked as ✗). Besides, they do not support APE by themselves.

**(2) Deep Set based methods.** Deep Set based methods (Wang et al., 2020b; Li et al., 2021) modify the network architecture and rely on a shared embedding function  $\phi(x_i)$  to ensure API. Thus, their representation capacities are limited. Besides, they do not support APE as well.

**(3) GNN and Transformer based methods.** GNN (Jiang et al., 2018; Liu et al., 2020) and Transformer (Hu et al., 2021b) based methods are similar. They both rely on shared embedding functions, e.g., query/key/value functions, and similar neighbor aggregation functions, e.g., mean pooling or weighted attention, to achieve API and APE. And Transformer could be considered as a special case of Graph Attention Network (Veličković et al., 2018) (a kind of GNN). Note that previous MARL methods (Jiang et al., 2018; Liu et al., 2020) only apply GNN to achieve API but not APE.

**(4) API-DPN and API-HPN.** Both our API-DPN and API-HPN do not rely on the shared embedding function to ensure API and APE and thus the representation capacities are not limited. When applying API-DPN, we do not need to modify the network architectures of the underlying learning algorithms. But we may face the inconsistent issue for some special input cases as mentioned in the end of Section 5.1. Instead, API-HPN is more consistent and flexible while also ensure the model’s representation capacity, and thus is our preferred solution to achieve API and APE.

## 8. Conclusion and Future Work

In this paper, we propose two architectures that are both permutation invariant and permutation equivariance. They can be combined with most of the existing MARL algorithms to significantly improve the sample efficiency and the converged performance of these algorithms. It is noteworthy that although we only test our methods in fully cooperative settings, our approaches are very general and can be applied to competitive settings as well. Furthermore, we can not only apply the API designs to individual value function, but also to individual policy function, centralized value and policy functions, and even environment models. We consider all of these as our future work.

## References

- Battaglia, P. W., Hamrick, J. B., Bapst, V., Sanchez-Gonzalez, A., Zambaldi, V., Malinowski, M., Tacchetti, A., Raposo, D., Santoro, A., Faulkner, R., et al. Relational inductive biases, deep learning, and graph networks. *arXiv preprint arXiv:1806.01261*, 2018.
- Berner, C., Brockman, G., Chan, B., Cheung, V., Debiak, P., Dennison, C., Farhi, D., Fischer, Q., Hashme, S., Hesse, C., et al. Dota 2 with large scale deep reinforcement learning. *arXiv preprint arXiv:1912.06680*, 2019.
- Ha, D., Dai, A., and Le, Q. V. Hypernetworks. *arXiv preprint arXiv:1609.09106*, 2016.
- Hu, J., Jiang, S., Harding, S. A., Wu, H., and Liao, S.-w. Riit: Rethinking the importance of implementation tricks in multi-agent reinforcement learning. *arXiv preprint arXiv:2102.03479*, 2021a.
- Hu, S., Zhu, F., Chang, X., and Liang, X. Updet: Universal multi-agent reinforcement learning via policy decoupling with transformers. In *International Conference on Learning Representations*, 2021b.
- Hüttenrauch, M., Šošić, A., and Neumann, G. Guided deep reinforcement learning for swarm systems. *arXiv preprint arXiv:1709.06011*, 2017.
- Jang, E., Gu, S., and Poole, B. Categorical reparameterization with gumbel-softmax. *arXiv preprint arXiv:1611.01144*, 2016.
- Jiang, J., Dun, C., Huang, T., and Lu, Z. Graph convolutional reinforcement learning. *arXiv preprint arXiv:1810.09202*, 2018.
- Kalra, S., Adnan, M., Taylor, G., and Tizhoosh, H. R. Learning permutation invariant representations using memory networks. In *European Conference on Computer Vision*, pp. 677–693. Springer, 2020.
- Li, Y., Wang, L., Yang, J., Wang, E., Wang, Z., Zhao, T., and Zha, H. Permutation invariant policy optimization for mean-field multi-agent reinforcement learning: A principled approach. *arXiv preprint arXiv:2105.08268*, 2021.
- Littman, M. L. Markov games as a framework for multi-agent reinforcement learning. In *Machine learning proceedings 1994*, pp. 157–163. Elsevier, 1994.
- Liu, I.-J., Yeh, R. A., and Schwing, A. G. Pic: permutation invariant critic for multi-agent deep reinforcement learning. In *Conference on Robot Learning*, pp. 590–602. PMLR, 2020.
- Lowe, R., Wu, Y., Tamar, A., Harb, J., Abbeel, P., and Mordatch, I. Multi-agent actor-critic for mixed cooperative-competitive environments. *arXiv preprint arXiv:1706.02275*, 2017.
- Mena, G., Snoek, J., Linderman, S., and Belanger, D. Learning latent permutations with gumbel-sinkhorn networks. In *ICLR 2018 Conference Track*, volume 2018. OpenReview, 2018.
- Oliehoek, F. A. and Amato, C. *A concise introduction to decentralized POMDPs*. Springer, 2016.
- Rashid, T., Samvelyan, M., Schroeder, C., Farquhar, G., Foerster, J., and Whiteson, S. Qmix: Monotonic value function factorisation for deep multi-agent reinforcement learning. In *International Conference on Machine Learning*, pp. 4295–4304. PMLR, 2018.
- Rashid, T., Farquhar, G., Peng, B., and Whiteson, S. Weighted qmix: Expanding monotonic value function factorisation for deep multi-agent reinforcement learning. *Advances in Neural Information Processing Systems*, 33, 2020.
- Samvelyan, M., Rashid, T., De Witt, C. S., Farquhar, G., Nardelli, N., Rudner, T. G., Hung, C.-M., Torr, P. H., Foerster, J., and Whiteson, S. The starcraft multi-agent challenge. *arXiv preprint arXiv:1902.04043*, 2019.
- Santa Cruz, R., Fernando, B., Cherian, A., and Gould, S. Deeppermnet: Visual permutation learning. In *Proceedings of the IEEE Conference on Computer Vision and Pattern Recognition*, pp. 3949–3957, 2017.
- Santa Cruz, R., Fernando, B., Cherian, A., and Gould, S. Visual permutation learning. *IEEE transactions on pattern analysis and machine intelligence*, 41(12):3100–3114, 2018.
- Sarafian, E., Keynan, S., and Kraus, S. Recomposing the reinforcement learning building blocks with hypernetworks. In *International Conference on Machine Learning*, pp. 9301–9312. PMLR, 2021.
- Sunehag, P., Lever, G., Gruslys, A., Czarnecki, W. M., Zambaldi, V., Jaderberg, M., Lanctot, M., Sonnerat, N., Leibo, J. Z., Tuyls, K., et al. Value-decomposition networks for cooperative multi-agent learning. *arXiv preprint arXiv:1706.05296*, 2017.
- Vaswani, A., Shazeer, N., Parmar, N., Uszkoreit, J., Jones, L., Gomez, A. N., Kaiser, Ł., and Polosukhin, I. Attention is all you need. In *Advances in neural information processing systems*, pp. 5998–6008, 2017.
- Veličković, P., Cucurull, G., Casanova, A., Romero, A., Liò, P., and Bengio, Y. Graph attention networks. In

- International Conference on Learning Representations*, 2018.
- Vinyals, O., Babuschkin, I., Czarnecki, W. M., Mathieu, M., Dudzik, A., Chung, J., Choi, D. H., Powell, R., Ewalds, T., Georgiev, P., et al. Grandmaster level in starcraft ii using multi-agent reinforcement learning. *Nature*, 575 (7782):350–354, 2019.
- Wadhwan, S., Kim, D.-K., Omidshafiei, S., and How, J. P. Policy distillation and value matching in multiagent reinforcement learning. In *2019 IEEE/RSJ International Conference on Intelligent Robots and Systems (IROS)*, pp. 8193–8200. IEEE, 2019.
- Wagstaff, E., Fuchs, F., Engelcke, M., Posner, I., and Osborne, M. A. On the limitations of representing functions on sets. In *International Conference on Machine Learning*, pp. 6487–6494. PMLR, 2019.
- Wang, J., Ren, Z., Liu, T., Yu, Y., and Zhang, C. Qplex: Duplex dueling multi-agent q-learning. *arXiv preprint arXiv:2008.01062*, 2020a.
- Wang, W., Yang, T., Liu, Y., Hao, J., Hao, X., Hu, Y., Chen, Y., Fan, C., and Gao, Y. Action semantics network: Considering the effects of actions in multiagent systems. In *International Conference on Learning Representations*, 2019.
- Wang, W., Yang, T., Liu, Y., Hao, J., Hao, X., Hu, Y., Chen, Y., Fan, C., and Gao, Y. From few to more: Large-scale dynamic multiagent curriculum learning. In *Proceedings of the AAAI Conference on Artificial Intelligence*, volume 34, pp. 7293–7300, 2020b.
- Yang, T., Tang, H., Bai, C., Liu, J., Hao, J., Meng, Z., and Liu, P. Exploration in deep reinforcement learning: a comprehensive survey. *arXiv preprint arXiv:2109.06668*, 2021.
- Yang, Y., Hao, J., Liao, B., Shao, K., Chen, G., Liu, W., and Tang, H. Qatten: A general framework for cooperative multiagent reinforcement learning. *arXiv preprint arXiv:2002.03939*, 2020.
- Ye, Z., Chen, Y., Song, G., Yang, B., and Fan, S. Experience augmentation: Boosting and accelerating off-policy multi-agent reinforcement learning. *arXiv preprint arXiv:2005.09453*, 2020.
- Yu, C., Velu, A., Vinitsky, E., Wang, Y., Bayen, A., and Wu, Y. The surprising effectiveness of mappo in cooperative, multi-agent games. *arXiv preprint arXiv:2103.01955*, 2021.
- Zaheer, M., Kottur, S., Ravanbakhsh, S., Poczos, B., Salakhutdinov, R. R., and Smola, A. J. Deep sets. *Advances in Neural Information Processing Systems*, 30, 2017.
- Zhou, M., Luo, J., Villella, J., Yang, Y., Rusu, D., Miao, J., Zhang, W., Alban, M., Fadar, I., Chen, Z., et al. Smarts: Scalable multi-agent reinforcement learning training school for autonomous driving. *arXiv preprint arXiv:2010.09776*, 2020.



## A. Complete Experimental Results

### A.1. The Full Comparison of API-HPN with SOTA on SMAC (RQ1)

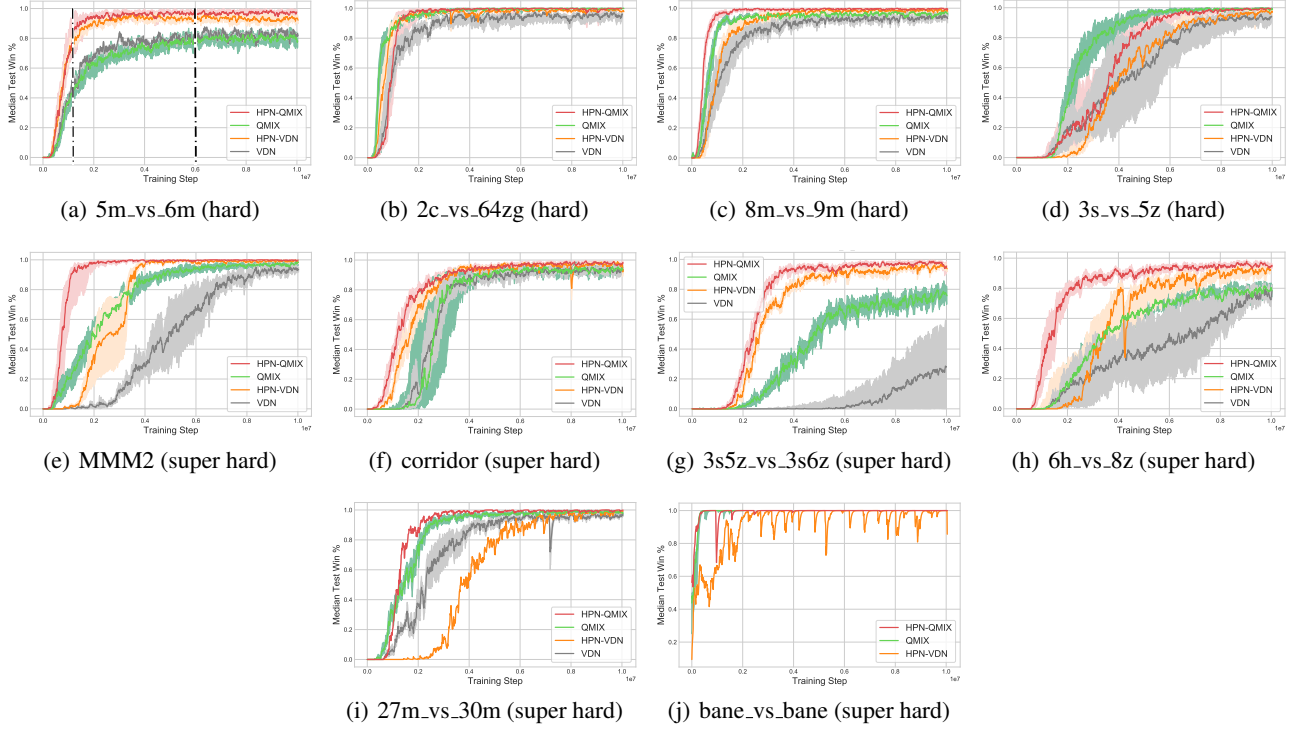


Figure 8. The learning curves of our HPN-QMIX and HPN-VDN compared with the SOTA fine-tuned QMIX and the fine-tuned VDN over all hard and super hard scenarios.

We compare our API-HPN with the SOTA fine-tuned QMIX (Hu et al., 2021a) and fine-tuned VDN over all hard and super hard scenarios. The learning curves are shown in Figure 8. Note that we do not extremely tune the hyperparameters for each scenario and use the same parameter settings across all scenarios instead. The detailed parameter settings are shown in Appendix C. From the figure, we conclude that:

- (1) Our HPN-QMIX surpasses the fine-tuned QMIX by a large margin and achieves 100% test win rates in almost all scenarios, especially in *5m\_vs\_6m*, *3s5z\_vs\_3s6z* and *6h\_vs\_8z* (never achieved before). Therefore, HPN-QMIX achieves the **new SOTA** on the SMAC benchmark;
- (2) Our HPN-VDN also significantly improves the performance of the fine-tuned VDN, and it even surpasses the fine-tuned QMIX in most scenarios and achieves close performance to the HPN-QMIX, which minimizes the gaps between the VDN-based and QMIX-based algorithms;
- (3) The sample efficiency of both HPN-VDN and HPN-QMIX is significantly improved, especially in *5m\_vs\_6m*, *MMM2*, *3s5z\_vs\_3s6z* and *6h\_vs\_8z*. An example is shown in Figure 5 (a), on *5m\_vs\_6m*, we mark 2 dotted lines in black to indicate the number of training steps needed to achieve the same 80% win rate of different algorithms. We see HPN-VDN and HPN-QMIX use much less samples by a factor of  $\frac{1}{4}$ .

### A.2. The Comparison of API-Networks with Related Baselines (RQ2 and RQ3)

#### A.2.1. Superiority of HPN-VDN to DPN-VDN (RQ2)

The results of the fine-tuned VDN equipped with API-HPN and API-DPN are shown in Figure 9, denoted as HPN-VDN and DPN-VDN respectively. As shown in Figure 9, (1) both HPN-VDN and DPN-VDN achieve superior performance, which validates the effectiveness of our API and APE designs; (2) HPN-VDN is more stable and achieves better win rates than DPN-VDN, especially in the *6h\_vs\_8z* scenario where DPN-VDN’s win rate is very low, which validates the robustness and superiority of our HPN design.

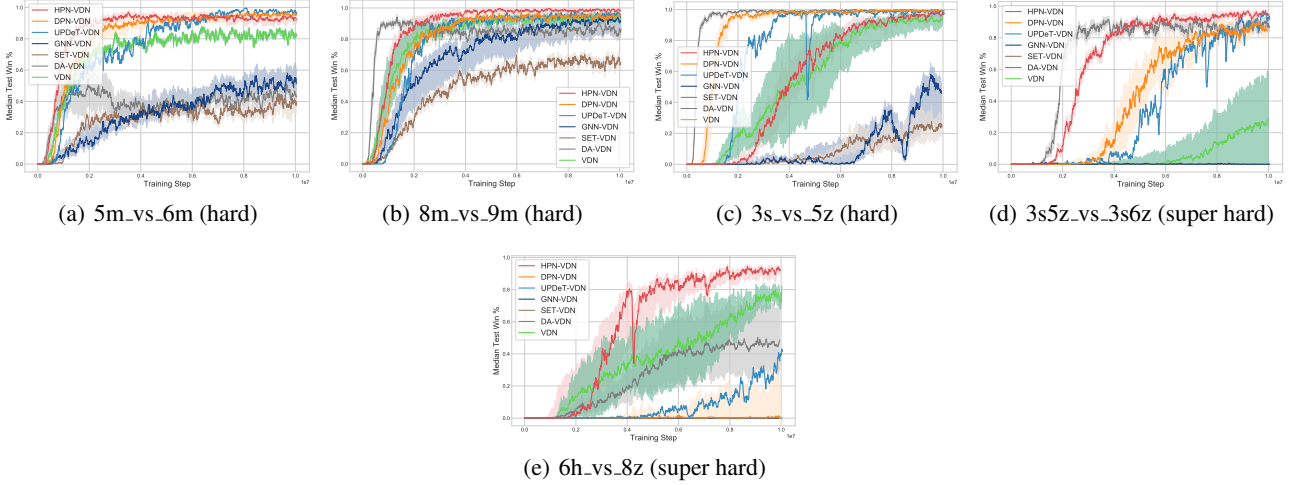


Figure 9. Comparisons of VDN-based methods considering the permutation invariance and equivariance.

### A.2.2. Comparison with Related VDN-based Baselines (RQ3)

The results are shown in Figure 9, which demonstrate that: (1) our HPN-VDN achieves the best win rates compared with other baselines; (2) EA-VDN significantly improves the learning speed and performance of vanilla VDN in *3s\_vs\_5z* and *3s5z\_vs\_3s6z* by experience augmentation and much more times of parameter updating. However, the learning process is unstable and collapses in all other scenarios due to the perturbation of the input features, which validates that it is hard to train a permutation-sensitive function (e.g., MLP) to output the same value when taking different orders of features as inputs. (3) GNN-VDN achieves slightly better performance than SET-VDN. Although permutation invariant is maintained, GNN-VDN and SET-VDN perform worse than vanilla QMIX, (especially on *3s5z\_vs\_3s6z* and *6h\_vs\_8z*, the win rates are approximate 0%). This confirms that the use of a shared embedding layer  $\phi(x_i)$  for each component  $x_i$  limits the representational capacities and restricts the final performance. (5) Since UPDeT uses a shared token embedding layer followed by multi-head self-attention layers to process all components of the input sets, the permutation invariant and permutation equivariant properties are implicitly taken into consideration. The results of UPDeT-VDN also validate that incorporating API and APE into the model design could reduce the observation space and improve the converged performance in most scenarios. However, due to the limited representational capacity of the shared token embedding layer, the performance of UPDeT-VDN is unstable, especially in *6h\_vs\_8z*.

### A.3. Ablation Studies (RQ4, RQ5, RQ6)

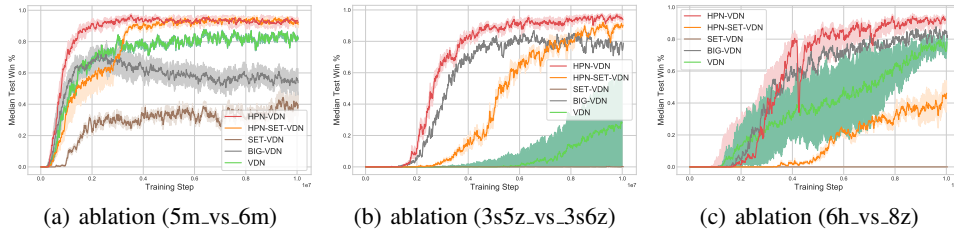


Figure 10. Ablation studies. All methods are equipped with VDN.

**(RQ4).** We also enlarge the agent network of vanilla VDN (denoted as BIG-VDN) such that the number of parameters is larger than our HPN-VDN. The detail number of parameters are shown in Table 2 of Appendix C. The results are shown in Figure 10. We see that simply increasing the parameter number cannot always guarantee better performance. For example, in *5m\_vs\_6m*, the win rate of BIG-VDN is worse than the vanilla VDN. In *3s5z\_vs\_3s6z* and *6h\_vs\_8z*, BIG-VDN does achieve better performance, which indicates that enlarging the network size in harder scenarios could stabilize training and achieve better performance. But the performance of BIG-VDN is still worse than our HPN-VDN in all scenarios.

**(RQ5).** To validate the importance of the permutation equivariant output layer, we also add the hypernetwork-based output layer of HPN to SET-VDN (denoted as HPN-SET-VDN). The results are shown in Figure 10. We see that incorporating an APE output layer could significantly boost the performance of SET-VDN, and that the converged performance of

Table 2. The agent-networks’ parameter sizes of BIG-VDN, BIG-QMIX and our HPN-VDN, HPN-QMIX

Parameter Size	BIG-VDN, BIG-QMIX	HPN-VDN, HPN-QMIX
5m_vs_6m	109.964K	72.647K
3s_vs_5z	108.555K	81.031K
8m_vs_9m	114.959K	72.839K
corridor	127.646K	76.999K
3s5z_vs_3s6z	121.487K	98.375K
6h_vs_8z	113.55K	76.935K

HPN-SET-VDN is superior to the vanilla VDN in 5m\_vs\_6m and 3s5z\_vs\_3s6z.

(RQ6). However, due to the limit representational capacity of the shared embedding layer of Deep Set, the performance of HPN-SET-VDN is still worse than our HPN-VDN, especially in 6h\_vs\_8z. Note that the only difference between HPN-VDN and HPN-SET-VDN is the input layer, e.g., using hypernetwork-based customized embeddings or a simply shared one. The results validate the importance of improving the representational capacity of the permutation invariant input layer.

## B. Technical Details

### B.1. Gumbel Softmax

Gumbel Softmax (Jang et al., 2016) is utilized to transfer a vector of real numbers to a vector of one-hot encoding while keeping the transformation differentiable. The Gumbel-Softmax distribution is a continuous distribution over the simplex that can approximate samples from a categorical distribution. Mathematically, given a vector of dimension of  $m$ , samples from the Gumbel-Softmax distribution is calculated according to

$$y_i = \frac{\exp((\log(p_i) + g_i)/\tau)}{\sum_{j=1}^m \exp((\log(p_j) + g_j)/\tau)} \quad \text{for } i = 1, \dots, m \quad (1)$$

where  $p_1, \dots, p_m$  are the class probabilities. A Generic Python code for a stable implementation of sampling from the Gumbel-Softmax distribution is shown in Figure 12. The ‘hard’ flag is used to transform the output sample into a one-hot vector by using the reparameterization trick.

### B.2. Gumbel Sinkhorn Layer

To solve the ‘Permutation Learning’ or ‘Matching Learning’ problem mentioned in Section 5.1, previous methods in Vision domain (Santa Cruz et al., 2017; Mena et al., 2018) usually use a Temperature-controlled Gumbel Sinkhorn layer to produce a doubly-stochastic matrix  $M$  to approximate the permutation matrix while keeping the computing process differentiable. The entries of  $M$  tend to be zero or one in the limit as the temperature approaches zero. Details about the Sinkhorn Layer can be found in (Mena et al., 2018).

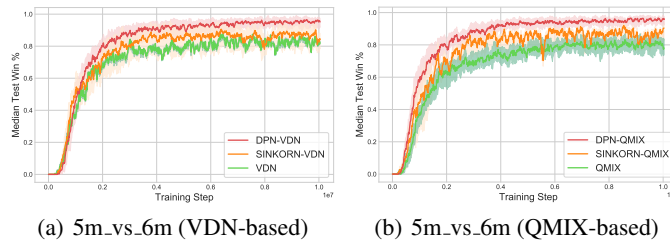


Figure 11. Ablation studies. Comparison Algorithm 1 with Gumbel Sinkhorn Layer.

However, in our settings, we found that our designed ‘Permutation Matrix Generation’ algorithm in Algorithm 1 achieves superior performance and behaves more robust than the previous Sinkhorn Layer. Learning curves of API-DPN equipped with both our designed Algorithm 1 and the Sinkhorn Layer in the 5m\_vs\_6m scenario are shown in Figure 11.



---

```

def sample_gumbel(shape, device, eps=1e-20):
    """Sample from Gumbel(0, 1)"""
    U = th.rand(*shape, device=device)
    return -th.log(-th.log(U + eps) + eps)

def gumbel_softmax_sample(logits, temperature):
    """ Draw a sample from the Gumbel-Softmax distribution"""
    y = logits + sample_gumbel(logits.shape, logits.device)
    return F.softmax(y / temperature, dim=-1)

def gumbel_softmax(logits, temperature=1.0, hard=False):
    """Sample from the Gumbel-Softmax distribution and optionally discretize.
    Args:
        logits: [batch_size, n_class] unnormalized log-probs
        temperature: non-negative scalar
        hard: if True, take argmax, but differentiate w.r.t. soft sample y
    Returns:
        [batch_size, n_class] sample from the Gumbel-Softmax distribution.
        If hard=True, then the returned sample will be one-hot, otherwise it will
        be a probability distribution that sums to 1 across classes
    """

    y = gumbel_softmax_sample(logits, temperature)
    if hard:
        y_hard = onehot_from_logits(y)
        y = (y_hard - y).detach() + y
    return y
    
```

---

Figure 12. A Generic Python code for a stable implementation of sampling from the Gumbel-Softmax distribution.

### B.3. Implementation of Baselines

The key points of implementing the baselines are summarized here:

(1) **Experience Augmentation (EA)** (Ye et al., 2020): we apply the core idea of Experience Augmentation (Ye et al., 2020) to SMAC by randomly generating a number of permutation matrices to shuffle the ‘observation’, ‘state’, ‘action’ and ‘available action mask’ for each sample simultaneously to generate more training data. An illustration of the Experience Augmentation process is shown in Figure 13. A noteworthy detail is that since the ‘attack actions’ are permutation equivariant to the enemies in the observation, the same permutation matrix  $M_2$  that is utilized to permute  $o_i^{\text{enemy}}$  should also be applied to permute the ‘attack action’ and ‘available action mask of attack action’ as well. The code is implemented based on PyMARL2<sup>4</sup> for fair comparison.

(2) **Deep Set** (Zaheer et al., 2017; Li et al., 2021): the only difference between SET-QMIX and the vanilla QMIX is that the vanilla QMIX uses a fully connected layer to process the fixedly ordered concatenation of the  $m$  components in  $o_i$  while SET-QMIX uses a shared embedding layer  $h_i = \phi(x_i)$  to separately process each component  $x_i$  in  $o_i$  first, and then aggregates all  $h_i$ s by sum pooling. The code is also implemented based on PyMARL2 for fair comparison.

(3) **GNN**: Following PIC (Liu et al., 2020), we apply GNN to the individual Q-network of QMIX (denoted as GNN-QMIX) to achieve permutation invariant. The code is also implemented based on PyMARL2.

(4) **ASN** (Wang et al., 2019): we use the official code and adapt the code to PyMARL2 for fair comparison.

(5) **UPDeT** (Hu et al., 2021b): we use the official code<sup>5</sup> and adapt the code to PyMARL2 for fair comparison.

All code of the baselines as well as our API Networks will be released latter.

<sup>4</sup><https://github.com/hijkzzz/pymarl2>

<sup>5</sup><https://github.com/hhhusiyi-monash/UPDeT>

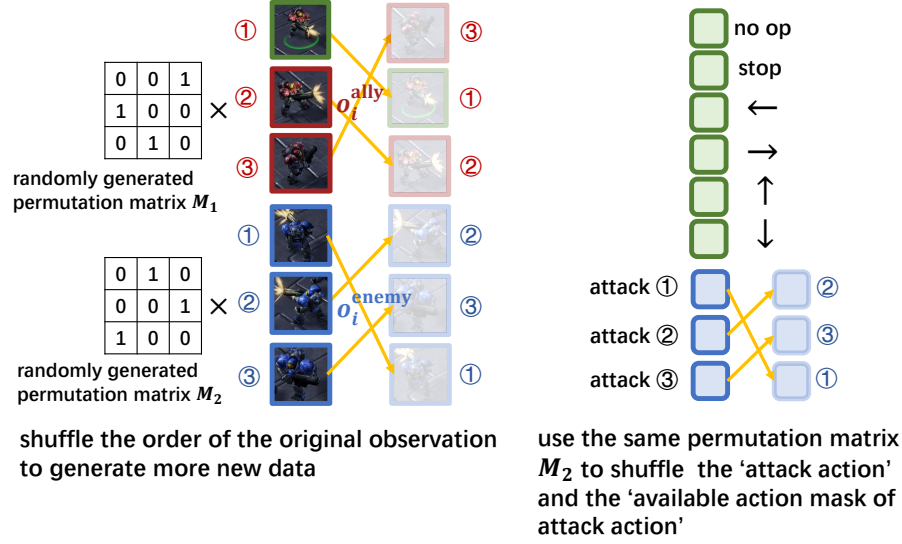


Figure 13. Apply Experience Augmentation (EA) to SMAC environment.

## C. Hyperparameter Settings

We list the detailed hyperparameter settings used in the paper bellow to help peers replicate our experiments more easily. Besides, all code of the baselines as well as our API Networks will be released latter.

### C.1. Hyperparameter Settings of VDN-based or QMIX-based Methods

Hyperparameter Settings of VDN-based or QMIX-based Methods are shown in Table 3.

### C.2. Hyperparameter Settings of MAPPO-based Methods

We use the default settings of the official open-sourced [MAPPO](https://github.com/marlbenchmark/on-policy)<sup>6</sup>. Hyperparameter Settings are shown in Table 4.

<sup>6</sup><https://github.com/marlbenchmark/on-policy>

Table 3. Hyperparameter Settings of VDN-based or QMIX-based Methods.

Parameter Name	Value
Exploration-related	
action_selector	epsilon_greedy
epsilon_start	1.0
epsilon_finish	0.05
epsilon_anneal_time	100000 (500000 for <i>6h_vs_8z</i> )
Sampler-related	
runner	parallel
batch_size_run	8 (4 for <i>3s5z_vs_3s6z</i> )
buffer_size	5000
t_max	10050000
Agent-related	
mac	hpn_mac for API-HPN, dpn_mac for API-DPN, set_mac for Deep Set, updet_mac for UPDeT and n_mac for others
agent	hpn_rnn for API-HPN, dpn_rnn for API-DPN, set_rnn for Deep Set, updet_rnn for UPDeT and rnn for others
HPN_hidden_dim	64 (only for API-HPN)
HPN_layer_num	2 (only for API-HPN)
permutation_net_dim	8 (only for API-DPN)
Training-related	
softmax_tau	0.5 (only for API-DPN)
learner	nq_learner
mixer	qmix or vdn
mixing_embed_dim	32 (only for qmix-based)
hypernet_embed	64 (only for qmix-based)
lr	0.001
td_lambda	0.6 (0.3 for <i>6h_vs_8z</i> )
optimizer	adam
target_update_interval	200



Table 4. Hyperparameter Settings of MAPPO-based Methods.

Parameter Name	Value
Environment-related	
add_agent_id	False
add_center_xy	True
add_distance_state	False
add_enemy_action_state	False
add_local_obs	False
add_move_state	False
add_visible_state	False
add_xy_state	False
Sampler-related	
n_rollout_threads	8
buffer_size	5000
num_env_steps	10050000
Actor-related	
actor_hidden_size	64
actor_net	vanilla
HPN_hidden_dim	64 (only for HPN-MAPPO)
lr	0.0005
share_policy	True
Critic-related	
critic_hidden_size	64
critic_lr	0.0005
Training-related	
clip_param	0.2
data_chunk_length	10
entropy_coef	0.01
gae_lambda	0.95
gain	0.01
gamma	0.99
huber_delta	10.0
ifi	0.1
max_grad_norm	10.0
num_mini_batch	1
opti_eps	1e-05
ppo_epoch	5
use_centralized_V	True
use_clipped_value_loss	True
use_eval	True
use_feature_normalization	True
use_gae	True
use_huber_loss	True
use_linear_lr_decay	False
use_max_grad_norm	True
use_mustalive	True
use_naive_recurrent_policy	False
use_obs_instead_of_state	False
use_orthogonal	True
use_policy_active_masks	True
use_popart	False
use_proper_time_limits	False
use_recurrent_policy	False
use_stacked_frames	False
use_state_agent	True
use_value_active_masks	False
use_valuenorm	True
value_loss_coef	1
weight_decay	0